Orbits in the H2O molecule

Efstathiou, K.; Contopoulos, G.

Published in:
Chaos

DOI:
10.1063/1.1356068

Publication date:
2001

Orbits in the H_2O molecule

K. Efstathiou, and G. Contopoulos

Citation: Chaos **11**, 327 (2001); doi: 10.1063/1.1356068
View online: https://doi.org/10.1063/1.1356068
View Table of Contents: http://aip.scitation.org/toc/cha/11/2
Published by the American Institute of Physics

Orbits in the H_2O molecule

K. Efstathiou and G. Contopoulos[a)]
Center for Astronomy, Academy of Athens, Anagnostopoulou 14, 106 73 Athens, Greece

(Received 16 August 2000; accepted 5 January 2001; published 30 March 2001)

We study the forms of the orbits in a symmetric configuration of a realistic model of the H_2O molecule with particular emphasis on the periodic orbits. We use an appropriate Poincaré surface of section (PSS) and study the distribution of the orbits on this PSS for various energies. We find both ordered and chaotic orbits. The proportion of ordered orbits is almost 100% for small energies, but decreases abruptly beyond a critical energy. When the energy exceeds the escape energy there are still nonescaping orbits around stable periodic orbits. We study in detail the forms of the various periodic orbits, and their connections, by providing appropriate stability and bifurcation diagrams.
 [DOI: 10.1063/1.1356068]

Small molecules are quantum systems, but their classical study reveals very important features. The method of the Poincaré surface of section plays a prominent role in such a study. A difficulty that appears often in realistic systems is that one cannot always choose a flat Poincaré surface of section that intersects all periodic orbits. In this paper we use a curved Poincaré surface of section in order to study a realistic model of the H_2O molecule. We find the phase plots for different values of the energy of the molecule. Then we find all the periodic orbits of period 1 and 2 and compute their stability and bifurcation diagrams.

I. INTRODUCTION

Two dimensional Hamiltonian systems are often studied using the technique of the Poincaré map, where one reduces the four dimensional, continuous time flow of the system to an associated *two dimensional* discrete map, by choosing an appropriate surface of section. Usually a flat surface of section is chosen and the orbits that cross this surface with a particular direction are the consequents of the Poincaré map.

For many systems a flat Poincaré surface of section (PSS) is not suitable since there are orbits of these systems that do not cross the surface of section. In these cases another choice must be made. In this paper we study a symmetric model of the H_2O molecule where we have chosen a curved PSS. This choice for the PSS permits us to study all the periodic orbits of the system for all the values of energy.

The study of periodic orbits and phase plots in realistic models of simple molecules, such as the model we are studying in this paper, gives interesting information that can be compared with the behavior of the corresponding quantum system and with experiments.[1,2] In particular the relation between classical periodic orbits and quantum mechanical eigenfunctions was emphasized by several authors, starting with the work of Gutzwiller.[3] The most surprising result was that in many cases one simple periodic orbit determines the basic form of the eigenfunction.[4–7] Further details can be found by using more periodic orbits[8] and the asymptotic structures around unstable periodic orbits.[9]

A partial study of periodic orbits in the H_2O molecule has been done by Lawton and Child,[10,11] Jaffé and Brumer,[12] and by Kellman,[13] who emphasize the bifurcation of the local stretching modes from the normal stretching vibrational mode. These papers contain references to previous work on orbits in the H_2O molecule.

We describe the model of the H_2O molecule in Sec. II, and use a convenient set of coordinates in defining the Hamiltonian. We calculate the equipotential surfaces for the symmetric molecule (Sec. III) and in Sec. IV we define an appropriate PSS and discuss its properties.

Then we study in detail the phase plots on such a PSS and find the main islands of stability and the chaotic zones (Sec. V). We calculate the main periodic orbits and their bifurcations and stability in Sec. VI. Finally we summarize our conclusions in Sec. VII.

II. A MODEL FOR THE H_2O MOLECULE

For the study of the H_2O molecule we have chosen a simple model that is well suited for classical calculations.[14] The potential energy has the form

$$V_{\mathrm{HHO}}=V_{\mathrm{O}}^{(1)}\cdot f(R_1,R_2,R_3)+V_{\mathrm{OH}}^{(2)}(R_1)+V_{\mathrm{OH}}^{(2)}(R_2)+V_{\mathrm{HH}}^{(2)}(R_3)+V_{\mathrm{HHO}}^{(3)}(R_1,R_2,R_3), \tag{1}$$

where R_1, R_2, and R_3 are the O–H_1, O–H_2, and H_1–H_2 distances, respectively. Distances are measured in Å and energies in eV. The single-body term in Eq. (1) is given by

$$V_{\mathrm{O}}^{(1)}\cdot f(R_1,R_2,R_3)=1.958\cdot\frac{1}{2}\left[1-\tanh\left(\frac{3\rho_3-\rho_1-\rho_2}{2}\alpha\right)\right], \tag{2}$$

where $\alpha=1.9018$, $\rho_1=R_1-0.9572$, $\rho_2=R_2-0.9572$, and $\rho_3=R_3-1.5139$. The two-body terms are given by the equations

$$V_{\mathrm{OH}}^{(2)}(R_i)=-D_1(1+a_1r_i+a_2r_i^2+a_3r_i^3)\exp\{-a_1r_i\},\quad i=1,2 \tag{3}$$

a)Electronic mail: gcontop@cc.uoa.gr

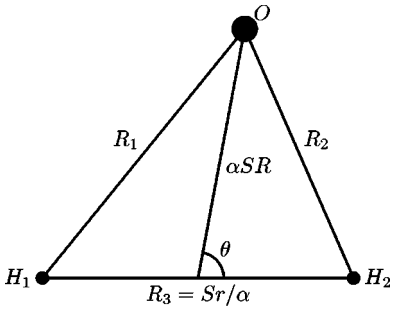

FIG. 1. Coordinates for the H_2O molecule.

where $r_i=R_i-0.9696$, $a_1=4.507$, $a_2=4.884$, $a_3=3.795$, and $D_1=4.6211$,

$$V_{\mathrm{HH}}^{(2)}(R_3)=-D_2(1+a_4r_3+a_5r_3^2+a_6r_3^3)\exp\{-a_4r_3\}, \tag{4}$$

where $r_3=R_3-0.7414$, $a_4=3.961$, $a_5=4.064$, $a_6=3.574$, and $D_2=4.7472$. Finally the three-body term is given by

$$V_{\mathrm{HHO}}^{(3)}(R_1,R_2,R_3)=0.018\,92\cdot P(\rho_1,\rho_2,\rho_3)\times\prod_{i=1}^{3}(1-\tanh(\gamma_i\rho_i/2)), \tag{5}$$

where $\gamma_1=\gamma_2=2.6$, $\gamma_3=1.5$, and $P(\rho_1,\rho_2,\rho_3)$ is the polynomial

$$P(\rho_1,\rho_2,\rho_3)=1+\sum_{i=1}^{3}C_i\rho_i+\sum_{i=1}^{3}\sum_{j=i}^{3}C_{ij}\rho_i\rho_j+\sum_{i=1}^{3}\sum_{j=i}^{3}\sum_{k=j}^{3}C_{ijk}\rho_i\rho_j\rho_k+\sum_{i=1}^{3}\sum_{j=i}^{3}\sum_{k=j}^{3}\sum_{l=k}^{3}C_{ijkl}\rho_i\rho_j\rho_k\rho_l. \tag{6}$$

The coefficients C_i, C_{ij}, C_{ijk}, and C_{ijkl} are defined in the paper by Murrell and Carter.[14]

Instead of the original coordinates R_1, R_2, and R_3 we will use the scaled Jacobi coordinates SR, Sr, θ (Fig. 1) that are defined by the equations

$$\mathrm{SR}=\frac{1}{2\alpha}\sqrt{2R_1^2+2R_2^2-R_3^2},\qquad \mathrm{Sr}=\alpha R_3,\qquad \cos\theta=\frac{R_2^2-R_1^2}{2\alpha\,\mathrm{SR}\,R_3}, \tag{7}$$

where α is given by the relation

$$\alpha=\left\{\frac{m_{\mathrm{O}}+2m_{\mathrm{H}}}{4m_{\mathrm{O}}}\right\}^{1/4}. \tag{8}$$

The inverse relations are

$$R_1=\sqrt{\left(\frac{\mathrm{Sr}}{2\alpha}\right)^2+(\alpha\,\mathrm{SR})^2-\mathrm{SR}\,\mathrm{Sr}\cos\theta},\qquad R_2=\sqrt{\left(\frac{\mathrm{Sr}}{2\alpha}\right)^2+(\alpha\,\mathrm{SR})^2+\mathrm{SR}\;\;\mathrm{Sr}\cos\theta}, \tag{9}$$

$$R_3=\frac{\mathrm{Sr}}{\alpha}.$$

The potential function given by Eqs. (1)–(6) can be written in scaled Jacobi coordinates using Eqs. (9).

The kinetic energy of the H_2O molecule has the form

$$T=\frac{1}{2\mu}\left[P_{\mathrm{SR}}^2+P_{\mathrm{Sr}}^2+\left(\frac{1}{\mathrm{SR}^2}+\frac{1}{\mathrm{Sr}^2}\right)P_\theta^2\right], \tag{10}$$

where P_{SR}, P_{Sr}, and P_θ are the conjugate momenta of SR, Sr, and θ, respectively. The parameter μ is defined by the relation

$$\mu=\sqrt{\frac{m_{\mathrm{O}}m_{\mathrm{H}}^2}{m_{\mathrm{O}}+2m_{\mathrm{H}}}}=\frac{m_{\mathrm{H}}}{2\alpha^2}. \tag{11}$$

The Hamiltonian can now be written as the sum of the kinetic and potential energies

$$H(P_{\mathrm{SR}},P_{\mathrm{Sr}},P_\theta,\mathrm{SR},\mathrm{Sr},\theta)=T(P_{\mathrm{SR}},P_{\mathrm{Sr}},P_\theta,\mathrm{SR},\mathrm{Sr})+V_{\mathrm{HHO}}(\mathrm{SR},\mathrm{Sr},\theta). \tag{12}$$

III. EQUIPOTENTIAL SURFACES

If we consider initial conditions with

$$\theta=\pi/2$$

and

$$P_\theta=0, \tag{13}$$

we can easily see that $\dot\theta=0$ and $\dot P_\theta=0$, meaning that the submanifold of the phase space determined by Eqs. (13) is invariant under the Hamiltonian flow and hence we can perform a standard type reduction in order to get a two degrees of freedom Hamiltonian system on this submanifold.

The reduced Hamiltonian $\tilde H$ is related to the original Hamiltonian through the relation

$$\tilde H(P_{\mathrm{SR}},P_{\mathrm{Sr}},\mathrm{SR},\mathrm{Sr})=H(P_{\mathrm{SR}},P_{\mathrm{Sr}},0,\mathrm{SR},\mathrm{Sr},\pi/2)=E \tag{14}$$

and its numerical value is the energy E of the molecule. This Hamiltonian describes the symmetric water molecule, where the distances $O-H_1$ and $O-H_2$ are equal.

The equipotential surfaces for the symmetric molecule are shown in Fig. 2. The potential has two minima at $\mathrm{SR}=\pm0.676\,065$, $\mathrm{Sr}=1.310\,82$, where it takes the value $E_0=-10.047$. Between the two minima there is a saddle point at $\mathrm{SR}=0$, $\mathrm{Sr}=1.6057$, where the potential takes the value $E_1=-8.993$. For $E<E_1$ orbits are confined inside the potential well around a minimum of the potential. For $E>E_1$ the two wells join and orbits can pass from one well to the other.

For values of energy greater than $E_2=-2.7892$ orbits can escape to infinity following the two horizontal channels at the left and the right of Fig. 2. Escape through these channels corresponds to a configuration of the molecule where the oxygen atom has become unbounded and the two hydrogen atoms form an H_2 molecule. Although for $E>E_2$ most orbits escape there are still bounded orbits as one can see in Fig. 6(c) below.

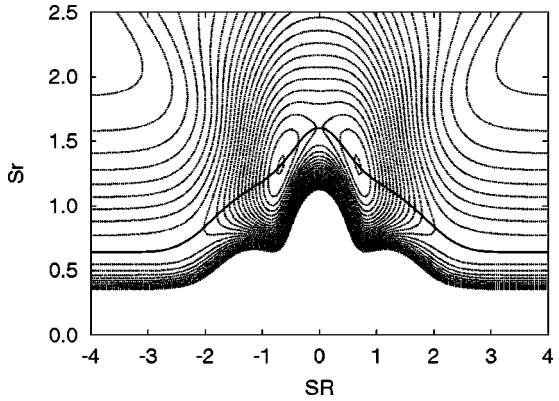

FIG. 2. Equipotential surfaces for the symmetric H_2O molecule. The solid line is the Poincaré surface of section.

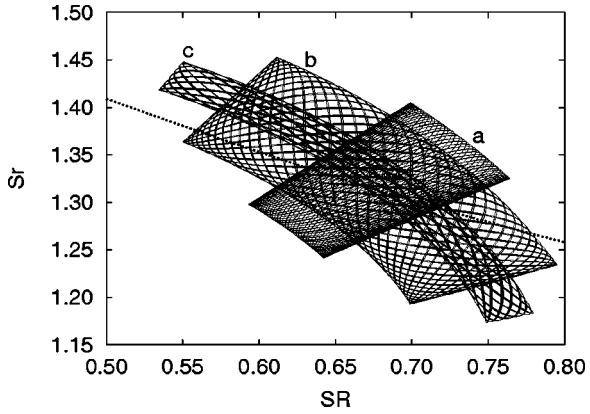

FIG. 4. Orbits *a* and *c* belong in the islands of 1*a* and 1*c*, respectively. The orbit *b* lies between these two islands. The thick line represents the PSS.

IV. A POINCARÉ SURFACE OF SECTION

A PSS should intersect almost all the orbits.[15] Such intersections occur naturally if the potential has a plane of symmetry. However this does not happen in the present case. On the other hand many orbits have a tendency to pass through a local minimum of the potential (although this is not always the case). Thus in order to find a suitable Poincaré surface of section we calculated numerically for each value of SR the corresponding value of Sr, where the potential function has a minimum. Then we fitted the numerically determined function $\mathrm{Sr}=f_{\mathrm{num}}(\mathrm{SR})$ by the analytic form

$$\mathrm{Sr}=f(\mathrm{SR})=\alpha\overline{f}(\alpha\mathrm{SR}), \tag{15}$$

where

$$\overline{f}(x)=0.740\,350+0.482\,392\exp(-3.342\,09x^2)+0.631\,258\exp(-0.112\,678x^4) \tag{16}$$

and α is given by Eq. (8).

This curve is given in Fig. 2. We determined that the difference between the numerically determined curve $\mathrm{Sr}=f_{\mathrm{num}}(\mathrm{SR})$ and the fitted analytic form is very small. For our computations we used the fitted form, given by Eqs. (15) and (16).

Contrary to the textbook approach we have not chosen SR and P_{SR} as the two coordinates on the PSS. If we had made such a choice we would have the following problem. Consider the orbits of Fig. 3. Both orbits cross the PSS at the same point with coordinates SR, Sr with the same momentum P_{SR} and they both have the same energy E. Then we solve Eq. (14) in order to determine P_{Sr}, and we get two solutions $\pm P_{\mathrm{Sr}}$. From Fig. 3 we can see that both solutions are valid, but they correspond to different orbits. This in turn means that on such a PSS different orbits would overlap and this is not permissible.

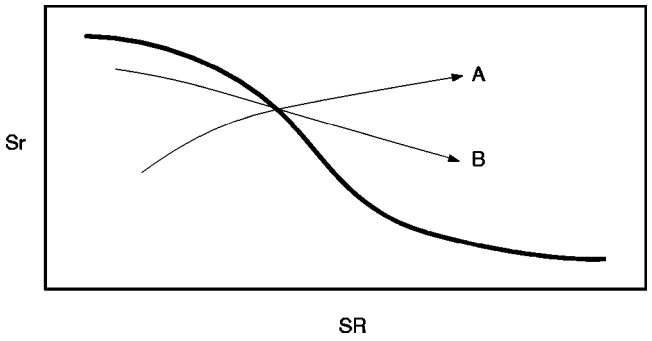

FIG. 3. The thick line gives the PSS. Orbits *A* and *B* cross the line at the same point with the same P_{SR} but opposite P_{Sr}.

In order to solve this problem we have chosen as coordinates on the PSS, SR and the component P_t of the momentum vector $P=(P_{\mathrm{SR}},P_{\mathrm{Sr}})$ tangential to the curve in Eq. (15). Thus the PSS is determined by the coordinate SR along the curve of Fig. 2 and the component P_t of the momentum. Some typical orbits on the plane (SR,Sr) are shown in Fig. 4.

A variable that is canonically conjugate to P_t is

$$Q_t=\int_0^{\mathrm{SR}}\sqrt{1+f'(x)}dx. \tag{17}$$

In fact the symplectic form in the variables Q_t, P_t is

$$\Omega=(dQ_t)\wedge(dP_t) \tag{18}$$

and it can be shown that this is preserved. The form Eq. (18) in the variables SR, P_t is written

$$\Omega=(1+f'(\mathrm{SR}))^{1/2}(d\mathrm{SR})\wedge(dP_t). \tag{19}$$

Thus the two-form $d\mathrm{SR}\wedge dP_t$ is not preserved in general. In our study we use the variable SR instead of Q_t because it is not practical to compute Q_t numerically.

Although the coordinates SR and P_t are not canonically conjugate, this does not cause any problems in the study of the system. In fact the integration is performed in the canonical coordinates SR, Sr, P_{SR}, P_{Sr} and the coordinates SR and P_t are used only on the PSS. The result is that the phase plots on the PSS are only slightly distorted relative to the phase plots that we would get if we had chosen canonically conjugate coordinates on the PSS.

V. PHASE PLOTS ON THE POINCARÉ SURFACE OF SECTION

In Figs. 5 and 6 we give the distribution of the orbits on the Poincaré surface of section for various values of the energy E.

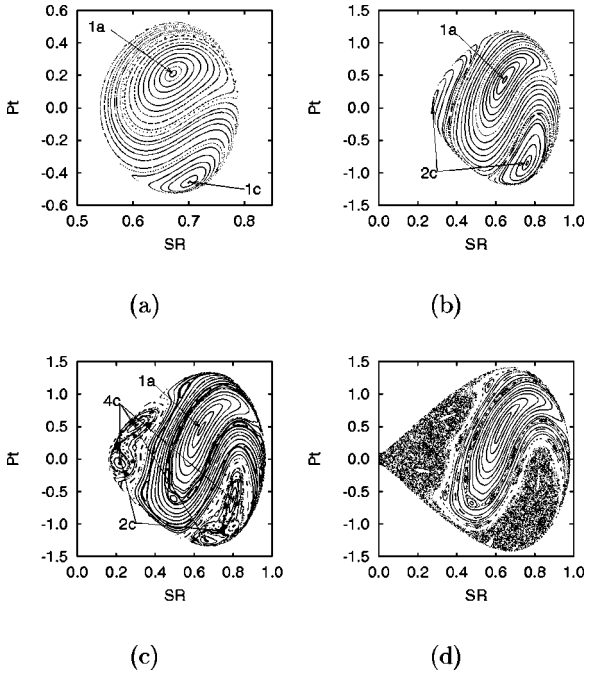

FIG. 5. Phase plots for small values of the energy: (a) $E=-9.9$, (b) $E=-9.3$, (c) $E=-9.1$, and (d) $E=-8.99$.

The energy of Fig. 5(a) is close to the minimum of the potential. In this plot practically all the orbits are ordered, defining closed invariant curves. Many invariant curves form two sets around two stable periodic orbits. The upper one is the orbit $1a$ and the lower one the orbit $1c$ (see Sec. VI). However there are also invariant curves between these two sets, that start on the left or upper side of the boundary, and terminate on the right side of the boundary. In Fig. 4 we can see why this is happening. In this figure we see three orbits for this value of the energy in configuration space. The orbits labeled as a and c belong to the islands of the periodic orbits $1a$ and $1c$, respectively. We see that the PSS crosses the outline of these orbits at two nonadjacent sides. When this is happening we get closed invariant curves on the PSS. But for the orbit labeled b, which lies between the two islands of Fig. 5(a), the PSS crosses the outline of this orbit at two adjacent sides (Fig. 4), and on the PSS we get an open invariant curve.

Figures 5(b), 5(c), and 5(d) refer to larger energies and are given in a larger scale than Fig. 5(a). Orbit $1c$ is continued as the double period orbit $2c$ in Fig. 5(b), the second point being near the left limit of the figure. The islands around both points $2c$ are now larger. In this case the chaotic orbits are also insignificant.

In Fig. 5(c) the orbit $2c$ is unstable (and is represented by two points at the centers of two dark regions) and it has produced four stable points by bifurcation that correspond to a stable orbit $4c$ of period 4, surrounded by islands of stability above and below each point of orbit $2c$. In this case there are some small chaotic zones around each unstable orbit.

The chaotic zones have grown considerably in Fig. 5(d). In this case there are still four islands of stability $4c$, as in Fig. 5(c), but very small. All the rest of the area previously occupied by bifurcations of orbit $2c$ and their corresponding islands are now chaotic. This case is just above the limiting value of the energy $E_1=-8.993$ at which the two potential wells join into one. Thus there is one symmetric figure for SR$<$0 that joins Fig. 5(d) at the small throat near the point (0,0). The point (0,0) represents orbit $1b$, which is unstable and produces a large chaotic region around it.

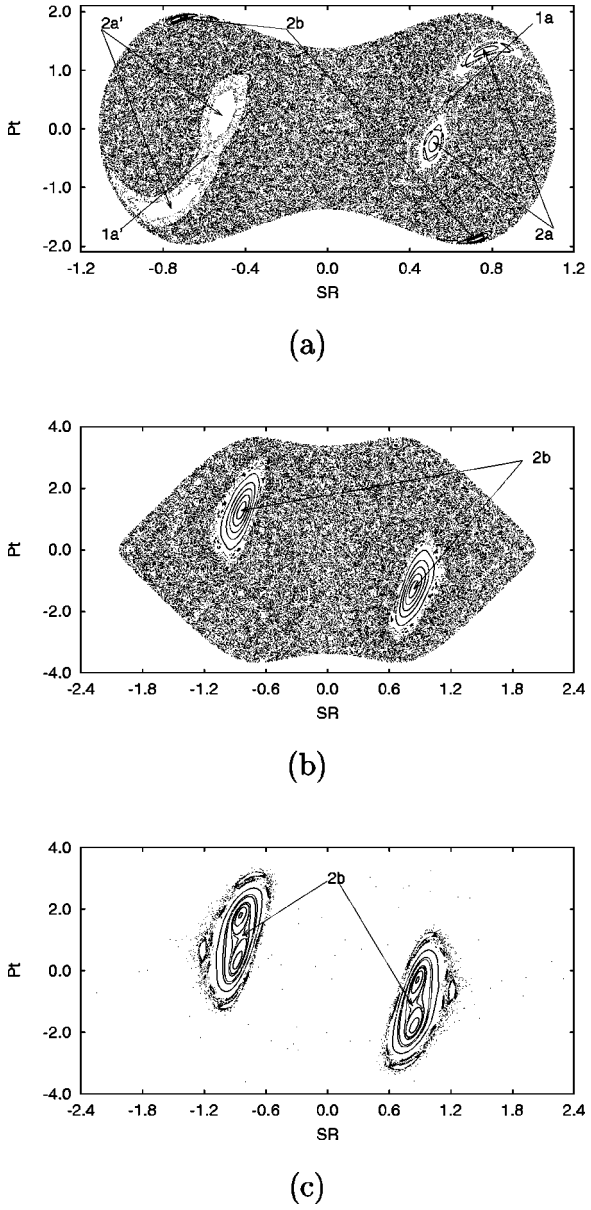

FIG. 6. Phase plots for energies: (a) $E=-8.0$, (b) $E=-3.0$, and (c) $E=-2.5$.

In Fig. 6(a) we give the phase plot for a larger value of the energy ($E=-8$) when the two potential wells are well connected at SR$=$0 (see the equipotentials of Fig. 2). Figure 6(a) is symmetric with respect to the axis SR$=$0. The apparent asymmetries in the islands of this figure are due to the use of nonsymmetric initial conditions on both sides of the axis SR$=$0. In this case orbit $1a$ is unstable and has generated by bifurcation orbit $2a$, surrounded by two islands of stability on the right half of Fig. 6(a). A symmetric orbit $1a'$ and its bifurcations $2a'$ appear on the left side of the figure.

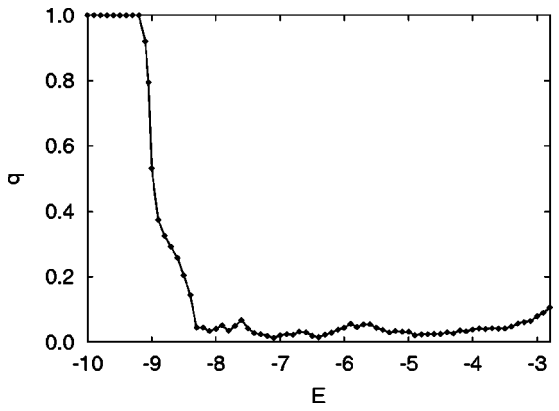

FIG. 7. Proportion of regular orbits, as a function of the energy E.

Orbits $1a$, $1a'$ have generated two chaotic domains that surround the islands $2a$ (respectively, $2a'$). At the lower left and upper right sides of this figure there are two elongated islands that belong to the family $2b$. The center of the figure (0,0) represents again the unstable orbit $1b$, which generates a large chaotic domain.

Most of Fig. 6(a) is covered by one chaotic orbit for which we have calculated $6 \cdot 10^4$ points. We see that the points of the chaotic orbit are not distributed uniformly on the PSS. This is a transient phenomenon and is due to stickiness of the orbits near cantori surrounding islands $2a$, or islands $2a'$. These cantori form partial barriers. Orbits need a long time in order to cross the cantori and for considerable times the regions inside and outside the cantori seem separated. This causes the apparent nonuniformity of the distribution of points on the PSS. But after a larger number of iterations the distribution of the points becomes uniform.

The phase plots for larger values of E have some similarity to Fig. 6(a) but there are also differences. For example, in Fig. 6(b) we see that there are two symmetric islands, one on each side of the axis SR=0. These islands belong to the irregular family $2b$, which is symmetric with respect to the point (0,0) (see Sec. VI), and not to two different families like families $1a$ and $1a'$ of Fig. 6(a). The chaotic domain in this case is again very large.

For E above the energy $E=E_2$ orbits can escape. In Fig. 6(c) we can see the islands around an orbit that belongs in family $2b$. The orbits that are outside these islands escape and this is why the area between the islands is empty.

The percentage of the area of the PSS covered by organized orbits as a function of the energy is presented in Fig. 7. We see that for values of energy close to $E_1=-10.047$ (the minimum value of the potential) almost all orbits are organized. An abrupt change happens at values of energy around $E=-9$. For $E>-9$ most of the PSS is filled by chaotic orbits. There are islands of stability for even larger values of the energy, and we notice that for values of the energy close to $E=-3$ the percentage of the organized orbits increases, although it remains below 0.2 (or 20%). This increase is due to the increase in the size of the island around family $2b$. The islands continue to increase in size even when E becomes larger than the escape energy $E_2=-2.79$, but for still larger E they become smaller.

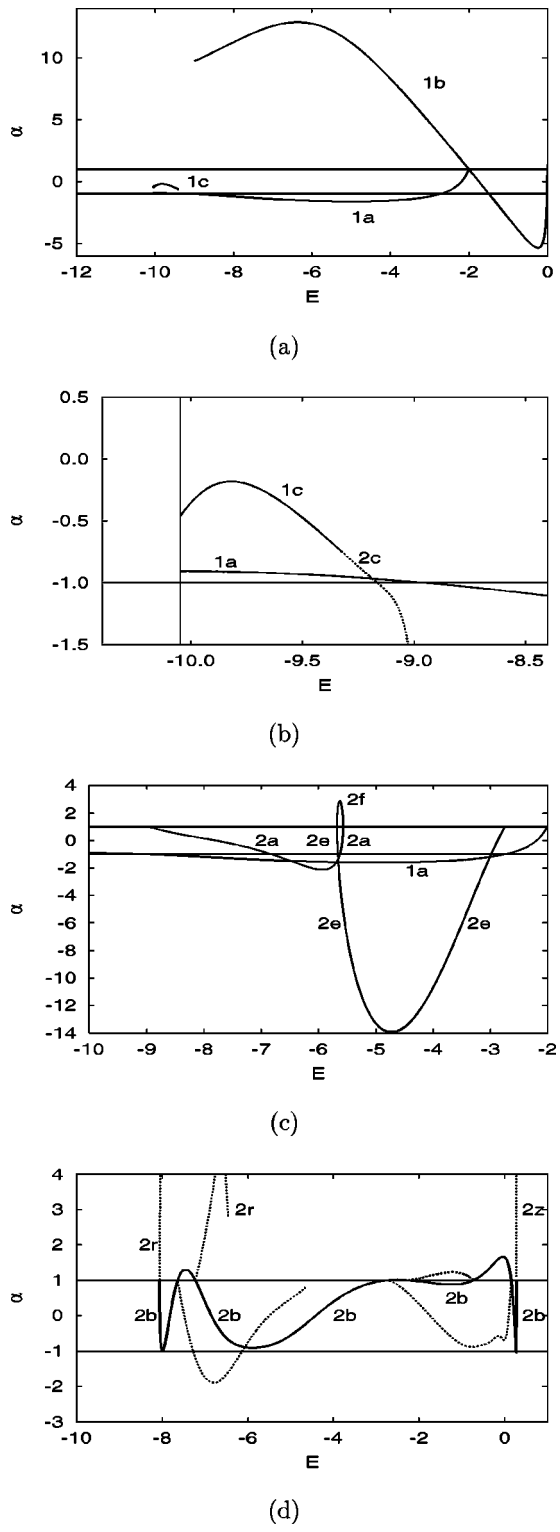

FIG. 8. Stability diagrams: (a) families $1a$, $1b$, $1c$, (b) families $1a$, $1c$, $2c$ (continuation of $1c$), (c) family $1a$ and its period 2 bifurcations, and (d) families $2b$, $2r$, $2z$.

VI. PERIODIC ORBITS

We have computed the most important families of periodic orbits for the symmetric water molecule. The stability diagram of the period-1 families as a function of the energy of the molecule can be seen in Fig. 8(a). Such a diagram gives the Hénon stability parameter[16] α of each family as a

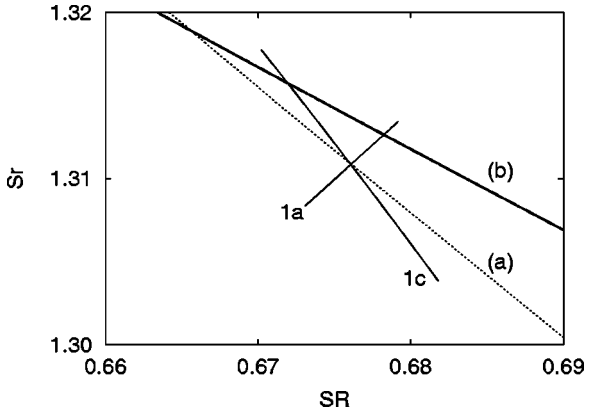

FIG. 9. Periodic orbits $1a$ and $1c$ for $E=-10.046\,64$ in configuration space. Line (a) represents the numerically determined minima of the potential and the line; (b) represents the selected PSS.

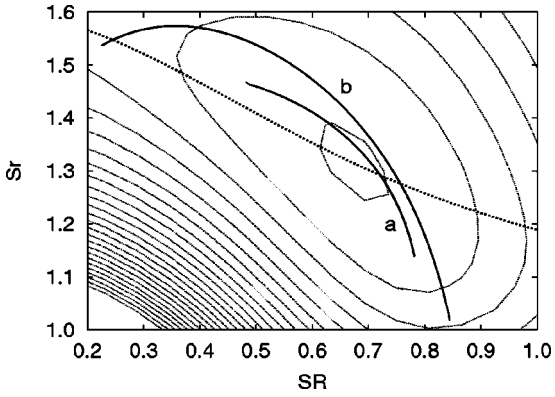

FIG. 10. The transition $1c\rightarrow 2c$. Orbit a ($E=-9.8$) belongs to family $1c$. Orbit b ($E=-9.2$) belongs to family $2c$.

function of E. For a period-k orbit of an area-preserving map σ, the Hénon stability parameter is defined by the relation

$$\alpha=\tfrac{1}{2}\mathrm{Trace}(D[\sigma^k](x_0)), \tag{20}$$

where x_0 is a point of the periodic orbit and $D[\sigma^k](x_0)$ is the Jacobian matrix of $\sigma\circ\cdots\circ\sigma$ (k times) evaluated at x_0. When the stability parameter of a periodic orbit lies in the interval from -1 to 1 the orbit is stable, otherwise it is unstable.

Since the Poincaré map is not symplectic, as we have explained in Sec. IV, the determinant of the Jacobian matrix $D\sigma(x)$ is not equal to 1 for arbitrary points x on the PSS. However for a periodic orbit with period k the determinant of $D[\sigma^k]$ is exactly equal to 1. In fact, using Eq. (19) it can be proven that the determinant of the Jacobian matrix of σ^k at a point $x_0=(\mathrm{SR}_0,P_{t0})$ is given by the relation

$$\det D[\sigma^k](x_0)=\sqrt{\frac{1+f'(\mathrm{SR}_0)}{1+f'(\mathrm{SR}_k)}}, \tag{21}$$

where $x_k=\sigma^k(x_0)=(\mathrm{SR}_k,P_{tk})$ is the kth image of x_0. If an orbit is periodic with period k, then $\mathrm{SR}_0=\mathrm{SR}_k$, hence $\det D[\sigma^k](x_0)=1$.

For values of energy close to the minimum value of the potential ($E=E_1=-10.047$) there exist two period-1 families. We call these families $1a$ and $1c$. They correspond to the two normal modes of the water molecule. In Fig. 9 we can see the corresponding periodic orbits at $E=-10.046\,64$ in configuration space.

Family $1c$ has a peculiar behavior that is the result of our choice of the PSS. This family is born at $E=-10.047$, but beyond the energy $E=-9.331$ it appears as a period-2 family, which we call $2c$ [Fig. 8(b)]. We note that no bifurcation appears here. In order to understand what is happening, we should see Fig. 10. In this figure we see one orbit of family $1c$ that intersects the PSS only at one point, as expected for small energies. An orbit of the same family for a larger value of the energy intersects the PSS at two points and thus it appears as a period-2 orbit. We will call the change of the apparent period of a family that is not related to a bifurcation, a *transition*. We note here that there would be a transition even if we had chosen, as the PSS, the numerically determined curve of the minima of the potential instead of the fitted function. Family $2c$ becomes unstable at $E=-9.164$ and generates by bifurcation two stable period 4 families.

For values of the energy between $E=E_1=-10.047$ and $E=-7.2$ the largest islands on the PSS are around family $1a$ and family $2a$, which bifurcate from $1a$ [Figs. 5 and 6(a)]. Family $1a$ is created at the minimum energy of the system $E=E_1=-10.047$ as a stable family and becomes unstable at $E=-8.95$ [Fig. 8(a)]. At this value of E it generates by bifurcation the period-2 family $2a$ [Fig. 8(c)]. Notice that when the stability parameter α of a period-1 orbit is equal to -1 the same orbit described twice has a stability parameter $+1$. Family $2a$ starts at $E=-8.95$ with stability parameter $\alpha=1$, and exists for larger values of E. Family $1a$ remains unstable until $E=-2.47$, where the period-2 family 2e is generated by bifurcation from family $1a$, existing for smaller values of E [Fig. 8(c)].

Family $2a$ for $E=-6.82$ becomes unstable by crossing the line $\alpha=-1$ and becomes stable again for $E=-5.62$. The stability parameter of family $2a$ takes the value $\alpha=1$ at $E=-5.568$. At this energy an unstable period-2 family, which we call $2f$, is created. Family $2e$ becomes unstable (going from larger to smaller values of the energy) for $E=-2.987$ and becomes stable again for $E=-5.661$. The stability parameter of family $2e$ takes the value $\alpha=1$ at $E=-5.675$. At this energy the unstable family $2f$, which was created at a larger energy from $2a$, joins $2e$ [Fig. 8(c)]. The bifurcation diagram of families $1a$, $2a$, $2e$, $2f$, $1b$ is shown in Fig. 11. This figure gives the value of SR for each energy. We see that family $2f$ exists only in a small interval of values of E and joins family $1a$ at its maximum E and family $2e$ at its minimum E. This explains why families $2a$, $2e$, and $2f$ form a loop in Fig. 8(c).

Between $E=-2.47$ and $E=-2.00$ family $1a$ remains stable. At $E=-2.00$ family $1a$ joins family $1b$, and for larger values of energy family $1a$ does not exist. We may thus say that family $1a$ is a bifurcation of family $1b$. Family $1b$ is represented by the point (0,0) on the surface of section. It is created at the energy $E_2=-8.993$ [Fig. 8(a)], at the saddle point of the potential (Fig. 2), with coordinates SR=0, Sr=1.6057. For energies somewhat larger than E_2

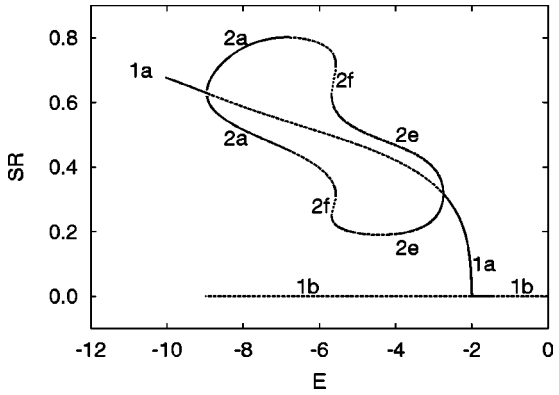

FIG. 11. Bifurcation diagram of family $1a$.

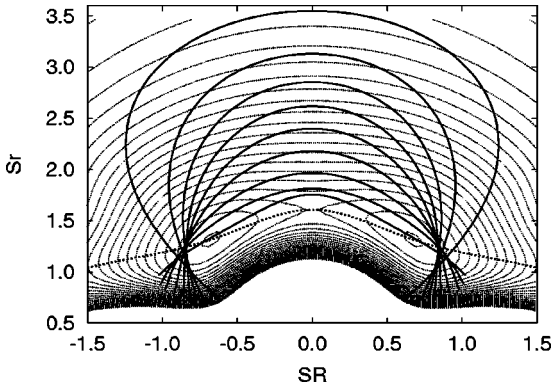

FIG. 13. Orbits of family $2b$ in configuration space. The dotted line represents the PSS.

family $1b$ is unstable ($\alpha=9.73$). As E increases, the stability parameter of family $1b$ becomes larger, but later (for larger E) it becomes smaller. At $E=-2.00$ this family becomes stable. It becomes unstable again at $E=-1.50$ with stability parameter $\alpha=-1$. For larger E family $1b$ is unstable, but at $E=-0.0205$ it becomes stable again until $E=-0.0110$, where it becomes unstable by crossing the line $\alpha=1$ and thus generating another period-1 family. As the energy approaches the energy $E=0$ the stability parameter of family $1b$ tends to infinity, and the return time (period) of the periodic orbit also tends to infinity.

In Fig. 12 we can see that periodic orbits of family $1b$ appear as straight lines in configuration space with SR=0 and varying Sr. In physical space this corresponds to a colinear configuration of the molecule with the oxygen atom in the middle and the two hydrogen atoms oscillating symmetrically at each side of the oxygen atom. For large intervals of the energy this configuration is unstable. In Fig. 12 we can also see how the periodic orbits of family $1a$ appear in configuration space for different values of the energy. We note that there is also a family $1a'$ that is symmetric to family $1a$ with respect to the axis SR=0. As the energy increases families $1a$ and $1a'$ approach family $1b$, and join $1b$ for $E=-2.00$.

At energy $E=-8.06$ two irregular period-2 families are created [Fig. 8(d)]. Irregular families are created in pairs (one stable and one unstable) by a tangent bifurcation. This

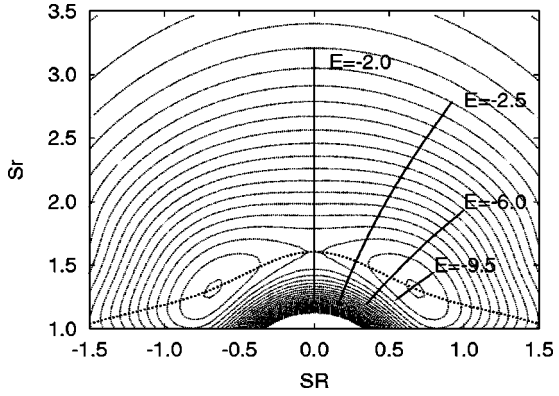

FIG. 12. Periodic orbits of families $1b$ (axis SR=0) and $1a$. The dotted line represents the PSS.

means that irregular orbits are not created by the bifurcation of an existing periodic orbit, but from each other. The stable family is called $2b$ and the unstable one is called $2r$. The stability parameter of family $2r$ grows from $\alpha=1$ to $\alpha=17.12$ as the energy increases and then decreases, until it reaches the value $\alpha=2.77$ at $E=-6.454$. For this energy family $2r$ appears as a period-4 family and we have a transition, as in the case of the transition $1c\rightarrow 2c$.

The stable family $2b$ plays an important role in the structure of the phase space. The stability diagram of family $2b$ and the period-2 families that bifurcate from $2b$ can be seen in Fig. 8(d). The diagram is very complex, much more than the stability diagram of family $1a$. Here we consider only family $2b$ and its equal period bifurcations. The stability parameter of family $2b$ crosses (or just reaches) the horizontal line $\alpha=1$ eight times. Each time this happens a family of period-2 orbits bifurcates from family $2b$. For $E=0.27$ family $2b$ joins a new unstable family $2z$ and they both disappear there, i.e., they do not exist for larger E.

Families $2b$, $2r$, and $2z$ are symmetric with respect to the point (0,0). The families that bifurcate from $2b$ are not symmetric but they come in symmetric pairs. In Fig. 8(d) some families that have bifurcated from family $2b$ suddenly terminate because they are going through transitions. Some orbits of family $2b$ can be seen in Fig. 13. In physical space these orbits correspond to oscillations of the oxygen atom between the two symmetric minima of the potential.

The island around the orbits of family $2b$ is the largest island for values of energy close to $E=-3$. Generally, from $E=-8$ to $E=-3$ the island around $2b$ occupies a significant measure of the PSS.

In the present paper we studied the stability (and instability) of the various types of orbits on the plane of symmetry $\theta=\pi/2$ and $P_\theta=0$. However orbits that are stable on this plane may be unstable in a direction perpendicular to this plane. An example is shown in Fig. 14, where we have calculated two stability parameters for family $2a$. One is the usual stability parameter α, as in Fig. 8(c), and the other is the stability parameter α_θ for deviations out of the symmetry plane. We see that while family $2a$ is stable with respect to deviation on the symmetry plane it becomes unstable with respect to perpendicular deviations for $E=-8$. At the transition to instability there is a bifurcation of a new period 2

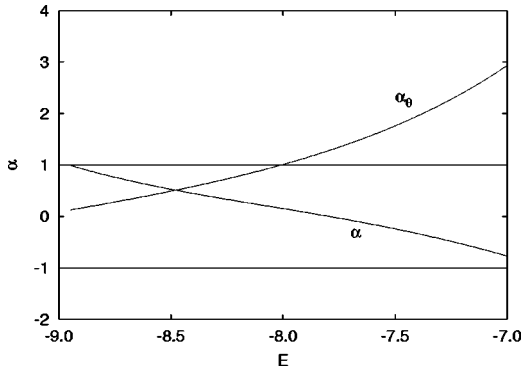

FIG. 14. Stability diagrams of the family *2a* for deviations on the symmetry plane (α) and perpendicular to it (α_θ).

family, which extends out of the symmetry plane and is initially stable.

The study of the stability of orbits in a direction out of the symmetry plane is important in many cases. Such studies in galactic dynamics have been made for a long time.[17] A detailed study of the stability and the bifurcations of periodic orbits with respect to the third dimension in the H_2O molecule will be given in a future paper.

VII. SUMMARY AND CONCLUSIONS

We have made a systematic study of the classical orbits for the symmetric configuration of a realistic model of the H_2O molecule. In order to study the distribution of the ordered and the chaotic orbits for this system, we had to choose an appropriate PSS. The usual choice for the PSS is a plane surface in phase space, but for the particular system studied here, this would not be convenient because for any choice of a plane PSS there would be important periodic orbits that would not cross it.

The PSS we chose is a surface passing approximately through the minima of the potential. Most nonescaping orbits cross this PSS. Choosing appropriate coordinates on this PSS, we were able to reduce the study of the dynamics of the symmetric H_2O molecule to the study of a two-dimensional map. With this particular choice of the PSS we ensure that the Poincaré map describes the complete dynamics of the molecule. A minor problem with this particular choice for the PSS is that some periodic families appear to change period without a bifurcation, due to an extra intersection of a periodic orbit with the PSS.

We found the distribution of the orbits on this PSS by distinguishing between ordered and chaotic orbits. The ordered orbits are represented by isolated points if they are periodic and by invariant curves if they are quasiperiodic. Most orbits are ordered for small energies. But as the energy increases beyond a critical value the proportion of ordered orbits decreases abruptly. When the energy increases beyond the escape energy ($E_2 = -2.7892$), most orbits escape to infinity, but there are still orbits trapped around stable periodic orbits. This remains true even when the energy increases above $E_3 = 0$, but for positive energies the regions of ordered motion are very small, and practically insignificant.

We studied the main periodic orbits of periods 1 and 2 for negative values of the energy. We constructed stability diagrams and bifurcation diagrams for the various families of periodic orbits. These diagrams are essential in understanding the role of various stable orbits in trapping nonperiodic orbits around them. In fact for different energies the trapping takes place around different orbits and we can separate the interval between the critical energy and the escape energy into two regions. In the first region (lower energies) the ordered orbits are trapped mainly around families $2a$ and $2a'$. In the second region, close to the escape energy the ordered orbits are trapped mainly around the irregular family $2b$.

ACKNOWLEDGMENTS

This research was supported by the Research Committee of the Academy of Athens (Grant No. 200/419). We thank Professor S. Farantos for his suggestion to use the particular model studied here. We also thank Dr. C. Skokos for useful discussions. K.E. has been supported in part by the Greek Foundation of State Scholarships (IKY). We also thank the (anonymous) referees for their remarks and for providing useful references.

[1] S. Farantos and M. Founargiotakis, Chem. Phys. **142**, 345 (1990).
[2] S. Keshavamurthy and G. Ezra, J. Chem. Phys. **107**, 156 (1997).
[3] M. Gutzwiller, J. Math. Phys. **12**, 343 (1971).
[4] E. Heller, E. Steckel, and M. Davis, J. Chem. Phys. **73**, 4720 (1980).
[5] M. Davis and E. Heller, J. Chem. Phys. **75**, 3916 (1981).
[6] S. Farantos and J. Tennyson, J. Chem. Phys. **82**, 800 (1985).
[7] M. Founargiotakis, S. Farantos, G. Contopoulos, and C. Polymilis, J. Chem. Phys. **91**, 1389 (1989).
[8] M. Berry, Proc. R. Soc. London, Ser. A **423**, 219 (1989).
[9] W. Schweizer, W. Jans, and T. Uzer, Phys. Rev. A **58**, 1382 (1998).
[10] R. Lawton and M. Child, Mol. Phys. **44**, 709 (1981).
[11] R. Lawton and M. Child, Mol. Phys. **37**, 1799 (1979).
[12] C. Jaffé and P. Brumer, J. Chem. Phys. **73**, 5646 (1980).
[13] M. Kellman, Annu. Rev. Phys. Chem. **46**, 395 (1995).
[14] J. Murrell and S. Carter, J. Phys. Chem. **88**, 4887 (1984).
[15] G. Birkhoff, *Dynamical Systems* (American Mathematical Society, New York, 1927).
[16] M. Hénon, Ann. Astrophys. **28**, 992 (1965).
[17] G. Contopoulos and P. Magnenat, Celest. Mech. **37**, 387 (1985).